

## STUDY OF CHROMATICITY CORRECTION IN LOW EMITTANCE STORAGE RING

M. Hara, R. Nagaoka, H. Tanaka\*, K. Tsumaki\*\*, K. Yoshida\*\*\*  
 RIKEN (The Institute of Physical and Chemical Research)  
 2-1, Hirosawa, Wako-shi, Saitama, 351-01, Japan

Abstract

An optimization method for the strength of sextupole magnets is studied and a computer program CATS (Correction of Amplitude-dependent Tune Shift) is developed. By applying this method to the design of 6 GeV storage ring in RIKEN SR Project [1], the dynamic aperture of the storage ring is remarkably enlarged and its effectiveness is confirmed.

Introduction

The low emittance lattice is generally characterized by its intrinsically large chromaticities. The large chromaticities result from the presence of the strong quadrupole magnets used to focus the charged particles especially at the dipole magnets. The linear part of chromaticities can be compensated by adding at least two families of sextupole magnets in the dispersive sections. These sextupoles, on the other hand, create harmful nonlinear effects (amplitude-dependent tune shift) on the large amplitude betatron motions and lead to substantial reduction of the dynamic aperture. To achieve sufficiently large dynamic aperture for the injection and for the long beam lifetime, other families of sextupoles must be introduced and their arrangement must be optimized. Thus, it is important to develop a method for the optimization. In this paper, we present a method for the optimization with a computer program CATS and show results of its application to our lattice design.

Theoretical foundation

The degree of amplitude dependence of the tunes is used to estimate harmful effects of the sextupoles on the betatron motions. Regarding sextupole fields as small perturbations, canonical perturbation theory [2-5] can be employed to describe the betatron motions with which the following "amplitude dependent tune shift formulae" are derived.

$$\Delta v_{xc} = C_{11} \cdot 2J_x + C_{12} \cdot 2J_y, \quad (1)$$

$$\Delta v_{yc} = C_{21} \cdot 2J_x + C_{22} \cdot 2J_y, \quad (2)$$

where

$$x = \sqrt{2J_x b_x} \cdot \cos\phi_x, \quad y = \sqrt{2J_y b_y} \cdot \cos\phi_y,$$

and  $J_x$  ( $J_y$ ) denotes the horizontal (vertical) action variable and  $\phi_x$  ( $\phi_y$ ) is the corresponding angle variable.

The suffix  $c$  in the tune shifts notifies that the analysis is made within a single cell. Four coefficients  $C_{ij}$  ( $i, j=1,2$ ) in Eqs. (1) and (2) are determined by the cell structure. These coefficients are expressed in the harmonic expansion,

$$C_{11} = -18 \cdot \sum_m [A_{3m}^2 / (3v_{xc-m}) + 3A_{1m}^2 / (v_{xc-m})], \quad (3)$$

$$C_{12} = C_{21} = +36 \cdot \sum_m [A_{1m} B_{1m} / (v_{xc-m}) - B_{+m}^2 / (v_{+c-m}) - B_{-m}^2 / (v_{-c-m})], \quad (4)$$

\* on leave from JGC Co.

\*\* on leave from Energy Research Laboratory, Hitachi Ltd.

\*\*\* on leave from Mitsubishi Electric Co.

$$C_{22} = -18 \cdot \sum_m [4B_{1m}^2 / (v_{xc-m}) + B_{+m}^2 / (v_{+c-m}) + B_{-m}^2 / (v_{-c-m})], \quad (5)$$

where

$$v_{\pm c} = v_{xc} \pm 2v_{yc}.$$

The summation with respect to  $m$  extends to  $-\infty < m < +\infty$ . Five additional coefficients  $A_{1m}$ ,  $A_{3m}$ ,  $B_{1m}$ , and  $B_{\pm m}$  in Eqs. (3)-(5) are composed of the sum of products of sextupole strength and betatron phase at the location of the sextupole magnets as follows;

$$A_{1m} = \sum_k (S_k / 48\pi) \cdot \cos(\psi_x - v_{xc}\theta + m\theta)_k, \quad (6)$$

$$A_{3m} = \sum_k (S_k / 48\pi) \cdot \cos[3(\psi_x - v_{xc}\theta) + m\theta]_k, \quad (7)$$

$$B_{1m} = \sum_k (S_{kb} / 48\pi) \cdot \cos(\psi_x - v_{xc}\theta + m\theta)_k, \quad (8)$$

$$B_{\pm m} = \sum_k (S_{kb} / 48\pi) \cdot \cos(\psi_{\pm} - v_{\pm c}\theta + m\theta)_k, \quad (9)$$

where

$$S_k = \{[\beta_x^{3/2} B''(y)L] / B\rho\}_k,$$

$$S_{kb} = \{[\beta_x^{1/2} \beta_y B''(y)L] / B\rho\}_k,$$

$$\psi_i = \int^c 1/\beta_i ds \quad (i = x, y), \quad \psi_{\pm} = \psi_x \pm 2\psi_y,$$

$$\theta = 2\pi \cdot (s/c), \quad c : \text{cell length}, \quad L : \text{sextupole length}.$$

As seen in the denominators of Eqs. (3)-(5), the first and third-order resonances driven by sextupoles are

$$v_{xc} = N, \quad (10)$$

$$3 \cdot v_{xc} = N, \quad (11)$$

$$v_{xc} \pm 2 \cdot v_{yc} = N, \quad (12)$$

where  $N$  is an arbitrary integer.

Optimization method

Basically, for a given lattice, the dynamic aperture is enlarged when the harmful resonance driving terms are sufficiently suppressed by introduction of additional sextupoles. To suppress the resonance driving terms, it must be considered that the distribution of the resonance driving terms depends greatly on the lattice structure and influences the optimum sextupole arrangement.

For example, if harmful resonance driving terms are localized in the vicinity of the working point per cell, they may be damped easily without raising  $|C_{ij}|$ . If, on the other hand, resonance driving terms in a wide range of  $m$  must be suppressed, it may not be so easy with few additional sextupoles. Therefore, one must make a careful observation of how they are distributed. As an effective tool for the observation, the program is developed to visualize resonance driving terms in various forms. Our method for optimization is described as follows:

Step-1

For a given lattice with only chromaticity correction sextupoles, the distribution of resonance driving terms, especially that in the vicinity of the working point, is checked.

Step-2

The resonance driving terms to be damped are selected

from the distribution and arrangement of additional sextupoles ( their initial strength and locations ) is determined.

#### Step-3

Selected resonance driving terms are suppressed with CATS.

#### Step-4

Dynamic aperture is checked. If sufficiently large dynamic aperture is obtained, the step for optimization is terminated here. If not, go on to the next step

#### Step-5

In the case that  $|C_{ij}|$  values are increased,  $|C_{ij}|$  multiplied by an appropriate weight function are added to the objective function of CATS and go back to Step-3.

Even though  $|C_{ij}|$  are decreased and selected resonance driving terms are damped, if the dynamic aperture is not enlarged, resonance driving terms which are far from the working point per cell are added step by step to the objective function of CATS and go back to Step-3

In the case that selected resonance driving terms are not damped, go back to Step-3 with the change in the sextupole arrangement or with introduction of other sextupoles. (Since the cancellation of resonance driving terms depends on the betatron phase at the sextupoles, it is useful to change sextupole locations or to introduce other sextupoles.)

#### Program CATS

For the given linear optics and the sextupole information, CATS optimizes the strength and locations of sextupoles. This program has following functions :

- (1)  $C_{ij}$  values are calculated from the distortion functions [5] and also the components of harmonic expansion of  $C_{ij}$  are calculated from the harmonic expansion formulae of amplitude dependent tune shifts, Eqs.(3)-(9).
- (2) Linear chromaticities are corrected with two specified families of sextupoles.
- (3) Strength of maximum twenty sextupoles per cell is optimized with an appropriate objective function.
- (4) If the sextupoles in the dispersive sections are used for optimization, the strength of chromaticity correction sextupoles is readjusted at every fitting loop automatically.

#### Applications

The above optimization method is applied to the design of two kinds of 6 GeV storage ring lattice, Chasman-Green (CG) lattice and Triple Bend Achromat (TBA) lattice. Lattice functions are depicted in Fig. 1(a) and 1(b).

In the case of CG lattice, harmonic expansion of  $C_{ij}$  has just one large peak at a component of  $m=1$  which is mainly composed of the first-order resonance ( $\nu_x=1$ ) driving term as shown in Fig. 2(a). Therefore, this peak is suppressed by CATS with only two families of sextupoles in the dispersion free sections. Though other components at positive side of  $m$  are newly excited, the component of  $m=1$  inducing the first-order resonance is suppressed completely as shown in Fig. 2(b). The dynamic aperture obtained before and after optimization is shown together in Fig. 3. The dynamic aperture is enlarged markedly after the optimization.

In the case of TBA lattice, harmonic expansion of  $C_{ij}$  has a few peaks near the working point and not only first but also third-order resonance driving terms are excited. For the suppression of complicated spectrum shown in Fig. 4(a), additional sextupoles are introduced in dispersive area to increase the degree of freedom for the optimization. With five families of harmonic sextupoles (including two sextupoles in dispersion free sections), all kinds of resonance driving terms from  $m = 1$  to  $m = 5$  in the vicinity

of the working point are adequately suppressed as shown in Fig. 4(b). Consequently, the dynamic aperture is enlarged for the TBA lattice as well, which is shown in Fig. 5.

The dynamic aperture not only of an ideal ring but also of a practical ring (the ring with magnetic errors) is studied for CG lattice. In this case, twofold optimization ( combination of the working point optimization and the sextupole arrangement optimization) is carried out. The optimal working point is searched by the tracking calculation changing the the tunes by small degrees around the desired working point. Due to the selection of appropriate working point, reduction of the dynamic aperture is minimized as shown in Fig. 6.

#### Summary

An optimization method for the strength of sextupole magnets is studied and a program CATS (Correction of Amplitude-dependent Tune Shift) is developed. In CATS, the coefficients describing the amplitude dependence of the tunes as well as their harmonic components are used as criteria of the optimization. Through its application to the design of two kinds of the low emittance lattice, CG lattice and TBA lattice, effectiveness of this method is confirmed.

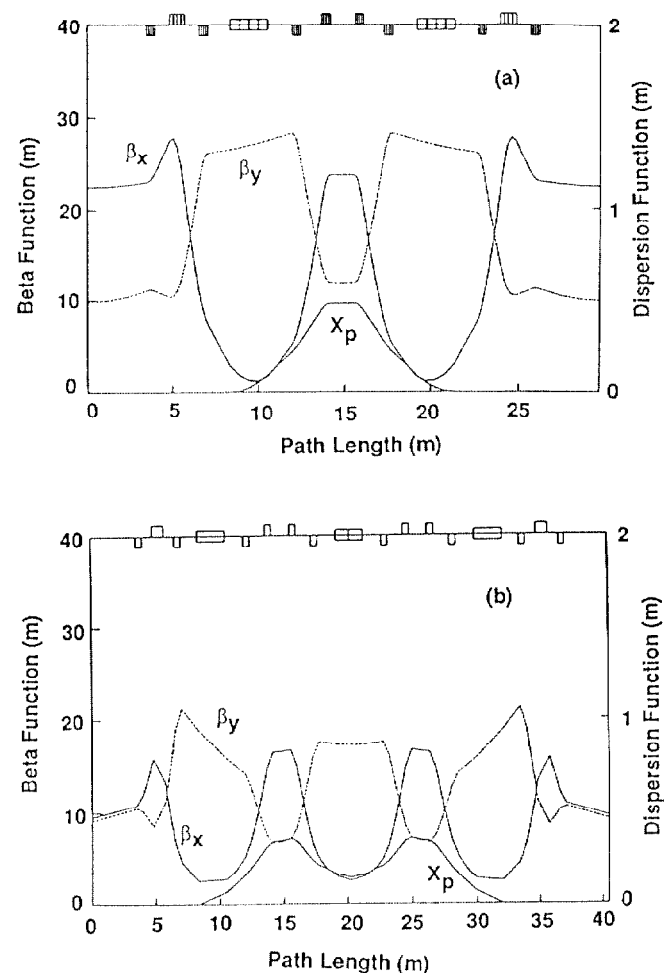


Fig. 1 Configuration of lattice functions  $\beta_x, \beta_y$ , dispersion function  $X_p$  for one cell. (a) CG lattice. (b) TBA lattice.

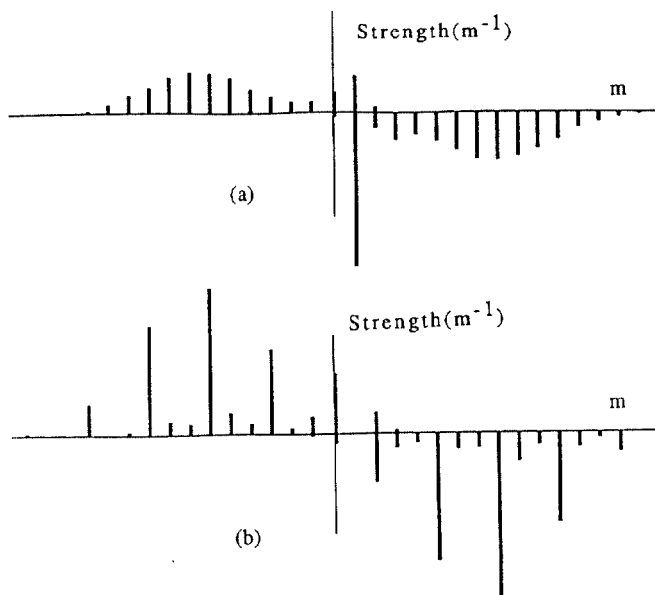


Fig. 2 Harmonic expansion spectrum of  $C_{ij}$  for CG lattice. (a) Before optimization. (b) After optimization.

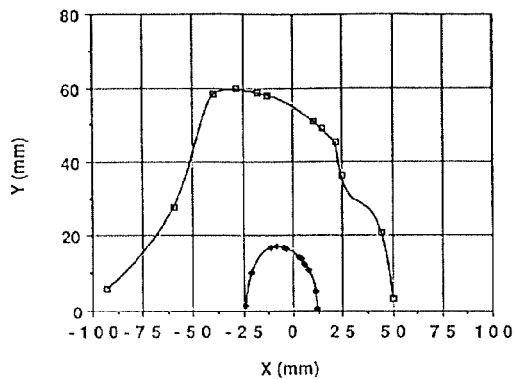


Fig. 3 Dynamic aperture of CG lattice obtained after optimization (white squares). For comparison, the dynamic aperture before optimization is also shown (dark squares).

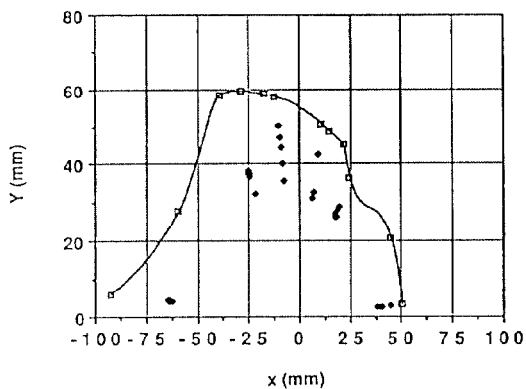


Fig. 6 Dynamic aperture of CG lattice in the presence of errors (dark squares). Calculation is made for five arbitrary machines. For comparison, the dynamic aperture of the ideal machine is also shown (white squares).

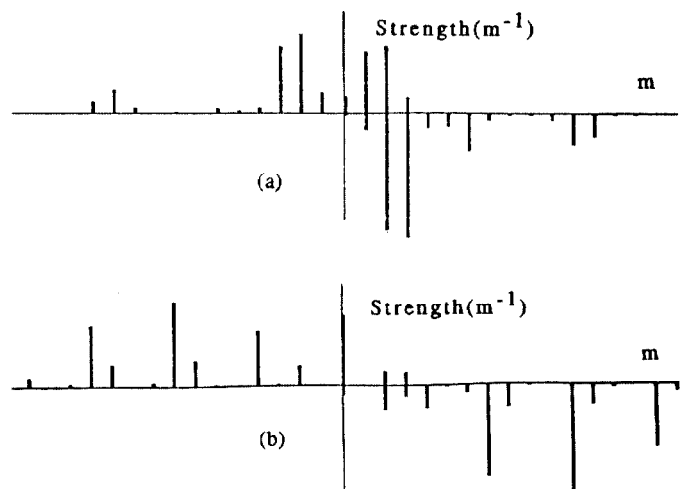


Fig. 4 Harmonic expansion spectrum of  $C_{ij}$  for TBA lattice. (a) Before optimization. (b) After optimization.

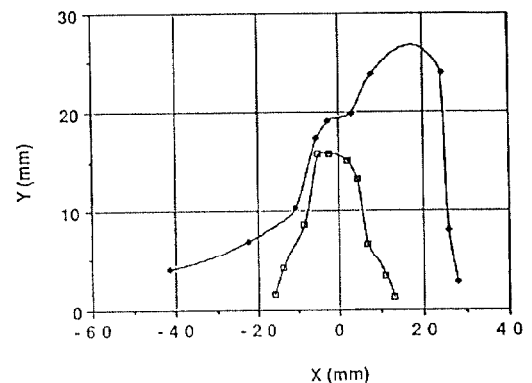


Fig. 5 Dynamic aperture of TBA lattice obtained after optimization (dark squares). For comparison, the dynamic aperture before optimization is also shown (white squares).

#### References

- [1] H. Kamitsubo, S. H. Be, M. Hara, R. Nagaoka, S. Sasaki, and T. Wada, "RIKEN SR Project", MP101 in this conference.
- [2] E. A. Crosbie, "Improvement of The Dynamic Aperture In Chasman Green Lattice Design Light Source Storage Rings", ANL-HEP-CP-87-21.
- [3] H. Wiedemann, "Chromaticity correction in large storage rings", PEP-220 (September 1976).
- [4] E. Courant, R. Ruth, and W. Weng, "Stability in Dynamical Systems I", Summer School on High Energy Particle Accelerators, Upton, NY (July 1983).
- [5] K.-Y. Ng, "Distortion Functions", Lecture given in KEK Oho'87 High Energy Accelerator Seminars (August 1987).